J Ginseng Res 42 (2018) 277–287

Contents lists available at ScienceDirect

Journal of Ginseng Research

journal homepage: http://www.ginsengres.org

Research article

Remarkable impact of steam temperature on ginsenosides transformation from fresh ginseng to red ginseng

Xin-Fang Xu [1], Yan Gao [1], Shu-Ya Xu [1], Huan Liu [1], Xue Xue [1], Ying Zhang [1], Hui Zhang [1], Meng-Nan Liu [1], Hui Xiong [1], Rui-Chao Lin [1,2], Xiang-Ri Li [1,2,*]

[1] School of Chinese Materia Medica, Beijing University of Chinese Medicine, Beijing, China
[2] Beijing Key Laboratory for Quality Evaluation of Chinese Materia Medica, Beijing University of Chinese Medicine, Beijing, China

ARTICLE INFO

Article history:
Received 12 November 2016
Accepted 20 February 2017
Available online 27 February 2017

Keywords:
MVA
red ginseng
steaming temperature
transformation
UPLC–QTOF-MS/MS

ABSTRACT

Background: Temperature is an essential condition in red ginseng processing. The pharmacological activities of red ginseng under different steam temperatures are significantly different.
Methods: In this study, an ultrahigh-performance liquid chromatography quadrupole time-of-flight tandem mass spectrometry was developed to distinguish the red ginseng products that were steamed at high and low temperatures. Multivariate statistical analyses such as principal component analysis and supervised orthogonal partial least squared discrimination analysis were used to determine the influential components of the different samples.
Results: The results showed that different steamed red ginseng samples can be identified, and the characteristic components were 20-gluco-ginsenoside Rf, ginsenoside Re, ginsenoside Rg1, and malonyl-ginsenoside Rb1 in red ginseng steamed at low temperature. Meanwhile, the characteristic components in red ginseng steamed at high temperature were 20*R*-ginsenoside Rs3 and ginsenoside Rs4. Polar ginsenosides were abundant in red ginseng steamed at low temperature, whereas higher levels of less polar ginsenosides were detected in red ginseng steamed at high temperature.
Conclusion: This study makes the first time that differences between red ginseng steamed under different temperatures and their ginsenosides transformation have been observed systematically at the chemistry level. The results suggested that the identified chemical markers can be used to illustrate the transformation of ginsenosides in red ginseng processing.

1. Introduction

Ginseng (*Panax ginseng* Meyer) is a famous traditional Chinese herb used for its medicinal properties and as a functional food to maintain balance in the human body in China, Korea, and Japan for more than 1,000 years [1,2]. Its bioactive ingredients include acidic polysaccharides, ginsenosides, proteins, and phenolic compounds [3–6].

In China, there are three kinds of ginseng according to their growth environment: cultivated ginseng, mountain cultivated ginseng, and mountain wild ginseng [7]. Cultivated ginseng is often processed into white ginseng, red ginseng, sugared ginseng, and active ginseng. Among these ginseng products, white ginseng and red ginseng are the most widely used in clinical applications because of their considerable pharmacological activity. Red ginseng is often used for "boosting yang" and replenishing vital essence with the "warming effect" [8]. Moreover, red ginseng exhibits more potential anticancer activity than white ginseng likely because of the abundant amount of rare ginsenosides generated from processing, such as ginsenosides Rg3 and Rh2 [9,10]. Traditionally, red ginseng is steamed at 90–100°C for 2–3 h and then dried until moisture qualified. The process condition directly influences the pharmacological activity of red ginseng. Research has revealed that the steaming temperature in red ginseng processing may affect the composition of ginsenosides, and the high steaming temperature could enhance the biological activity of red ginseng [11,12]. Thus, it is necessary to identify the chemical components present in red ginseng processed under different steaming temperatures and the "chemical marker" components between different processed samples to provide the chemical basis for the pharmacological activities.

Typically, ginsenosides are considered the main bioactive components, and they exhibit antioxidant, antiinflammatory,

* Corresponding author. School of Chinese Materia Medica, Beijing University of Chinese Medicine, Number 6 Wangjing Zhonghuannan Road, Beijing 100102, China.
E-mail address: lixiangri@sina.com (X.-R. Li).

http://dx.doi.org/10.1016/j.jgr.2017.02.003
p1226-8453 e2093-4947/$ – see front matter

anticancer, antiapoptotic, and immune-stimulant pharmacological activities [13–17]. According to different aglycones, ginsenosides can be classified into three types: protopanaxadiol type, such as ginsenoside Rb1, Rc, Rb2, and Rd; protopanaxatriol type, such as ginsenoside Rg1 and Re; and oleanolic acid type, which includes ginsenoside Ro and polyacetyleneginsenoside Ro [18]. Additionally, ginsenosides Rb1, Rb2, Rc, Rd, Re, and Rg1 are the most abundant ginsenosides in *P. ginseng*. The rest, which are the minority in *P. ginseng*, are called rare ginsenosides, and they also have significant pharmacological activities [19]. These ginsenosides can transform from one form to another during steam processing. Malonyl-ginsenosides, which are considered as an important form of ginsenosides in fresh ginseng, can demalonylate and transform to their corresponding ginsenosides upon processing. Some ginsenosides can deglycosylate into another ginsenoside; for example, ginsenosides Re, Rg1, Rd can deglycosylate into ginsenosides Rg2, Rh1, Rg3. Some ginsenosides can dehydrate into another ginsenoside; for example, ginsenosides Rg5, Rg6 are the dehydration products from ginsenosides Rg3, Rg2. Other ginsenosides such as Rs1 and Rs2 are the decarboxylization products of malonyl-ginsenoside Rb2 and malonyl-ginsenoside Rc. Moreover, the type of "S" ginsenosides that is the natural form existing in ginseng can transform into the type of "R" ginsenosides during the steaming process.

The ongoing development in ultrahigh-performance liquid chromatography (UPLC) coupled with MS-based metabolomics has the advantages of rapid analysis time, high resolution, selectivity, and sensitive analysis of components in complex medicinal herb mixtures. Recently, UPLC coupled with multivariate statistical analysis (MVA) was used to identify ginseng products, such as the commercial white and red ginseng [8], *P. ginseng* at different ages [20], white ginseng of different origins [21], and white ginseng, commercial red ginseng, and self-manufactured red ginseng [22]. These studies did not discuss the chemical changes of red ginseng processed at different steaming temperatures. However, the different marker components of red ginseng processed under different steaming temperatures have not been discovered. In our study, we developed a sample profiling strategy combining UPLC–quadrupole time-of-flight tandem mass spectrometry (UPLC–QTOF-MS/MS) and MVA as the analytical tools to compare the chemical contents of red ginseng at different steaming temperatures. This method allows us to understand the subtle differences between such ginseng products. At the same time, it can illuminate the transformation of ginsenosides into red ginseng at different steaming temperatures from the chemical components.

2. Materials and methods

2.1. Reagents

Fisher Optima grade acetonitrile, methanol, and isopropanol were purchased from Thermo Fisher Co. (Waltham, MA, USA). Formic acid and leucine enkephaline were purchased from Sigma Aldrich (St. Louis, MO, USA). Deionized water was obtained from our laboratory via a Milli-Q water purification system (Millipore Corporation, Bedford, MA, USA). Ginsenoside Rg1, Re, Rb1, Rf, Rb2, and Rb3 standards were purchased from the National Institute for the Pharmaceutical and Biological Products (Beijing, China). Ginsenoside Rc, Rg2 standards were obtained from Beijing Xiantong era Pharmaceutical Co. Ltd. (Beijing, China). The standards were dissolved in methanol and stored at 4°C.

2.2. Ginseng samples and sample processing

Twenty ginseng samples, which came from 6-year-old cultivated ginseng collected from Jingyu county, Jilin province, China, were used. All of these samples were fresh ginseng and then steamed at different temperatures. Red ginseng (HL) was made by steaming fresh ginseng at 100°C for 3 h, drying at 70°C for 12 h, and then drying until the water qualified at 50°C. Red ginseng (HH) was made by steaming fresh ginseng at 120°C for 3 h, drying at 70°C for 12 h, and then drying until the water qualified at 50°C.

All of these processed samples were identified by Professor Xiangri Li (School of Chinese Materia Medica, Beijing University of Chinese Medicine, Beijing, China) and deposited in the specimen cabinet of traditional Chinese medicine of Beijing University of Chinese Medicine.

2.3. Sample preparation

Fine roots of red ginseng samples processed at different steaming temperatures were pulverized to fine powder and sieved with 65 meshes. Then, accurately weighed powder (0.4 g) from each red ginseng powder was dissolved in 50 mL methanol, filled with plug, weighed, and ultrasonic extracted for 30 min. After cooling to room temperature, the weight loss was replenished with methanol and then filtrated. Then, with precision we drew subsequent filtrate (25 mL) and concentrated it into residue, which was then dissolved in methanol in a 10-mL volumetric flask. The extraction solution was injected into the UPLC system after being filtered through a 0.22-μm filter membrane.

2.4. Steaming model experiment

We performed the red ginseng steaming model experiment using ginsenoside Rb1. In the steaming model experiment, a certain amount of ginsenoside Rb1 was steamed at 100°C and 120°C for 3 h, respectively. After drying at 70°C for 12 h and then drying at 50°C, the residue was then dissolved in methanol in a 5-mL volumetric flask. Then after being filtered through a 0.45-μm filter membrane, this solution was injected into the high performance liquid chromatography (HPLC) system.

2.5. HPLC and UPLC–QTOF conditions

2.5.1. HPLC conditions

Changes in constituents via the steaming process were carried out using a Waters 2695 high performance liquid chromatograph coupled to a Waters 2489 detector with a C18 reversed phase column (250 mm × 4.6 mm, 5 μm) using the solvent gradient system. The mobile phase consisted of water (Solvent A) and acetonitrile (Solvent B), and the flow rate was 1 mL/min. The column oven temperature was set at 30°C. The gradient elution was used as follows: 0 min, 15% B; 10 min, 40% B; 25 min, 50% B; 38 min, 76% B. The total run time was 38 min, and the sample injection volume was 20 μL.

2.5.2. UPLC conditions

UPLC separation was performed on an ACQUITY UPLC system (Waters Corporation, Milford, MA, USA) with an ACQUITY UPLC BEH C_{18} column (100 mm × 2.1 mm, 1.7 μm). The column oven temperature was set at 40°C, and the flow rate was maintained at 400 μL/min. The mobile phase solvents A and B consisted of water with 0.1% formic acid and acetonitrile, respectively. The UPLC elution conditions were programmed as follows: 0–15 min (95–35% A), 15–18 min (35–0% A), 18–20 min (0–0% A), 20–22 min (0–95% A), 22–25 min (95–95% A). The total run time was 25 min, and the sample injection volume was 2 μL.

2.5.3. MS conditions

MS detection was performed on a quadrupole orthogonal acceleration time-of-flight tandem mass spectrometer (Waters

Synapt MS System). The data acquisition mode was MSE, and the ion polarity was set to negative mode (ESI^-). The optimized condition was as follows: source temperature was set at 110°C, desolvation gas flow was set at 600.0 L/h at a temperature of 500°C, and cone gas was set at 50 L/h. The lock mass compound used was leucine enkephaline, capillary and cone voltage was set at 2,200 V and 35 V, respectively. The collision energies were set as 20 eV for low-energy scan and 80 eV for high-energy scan. The UPLC–MS data acquisition was controlled by Mass Lynx 4.1 Mass Spectrometry Software (Waters Corporation).

2.6. Data processing procedure

Postacquisition data processing including the MVA was performed by Marker Lynx XS, which is an application manager for Mass Lynx software. The structural elucidation was performed using the Mass Fragment tool provided by Mass Lynx software.

2.6.1. Principal component analysis scores plot of samples

From the chromatographic trace, we obtained a three-dimensional (3-D) data point, which represents retention time, *m*/*z*, and intensity. It is necessary to convert each data point into an exact mass retention time (EMRT) pair by the Marker Lynx XS software. Once the EMRT 2-D matrix is obtained, the MVA interface will be launched with all EMRT information automatically imported so that the extended statistics module principal component analysis (PCA) can be carried out.

2.6.2. Scatter plot from orthogonal partial least squared discrimination analysis

We can also acquire the loading plot (S-plot) of every group pairs by orthogonal partial least squared discrimination analysis (OPLS-DA). In the S-plot, the leading contributing EMRT pairs can be captured selectively so that a list of top contributing markers from each sample group can be generated and saved as a text file.

2.6.3. Elemental composition calculation for the targeting markers

We used the exact mass of markers to calculate the matched elemental composition and search against an existing database for acquiring the chemical structure. Once the identity of a marker was tentatively identified, we could go back to the raw data file to investigate the fragment ions of samples in the high capillary electrophoresis scan. The fragment ions that we obtained using Mass Lynx can be used for elucidating the structure.

3. Results and discussion

3.1. UPLC-MS analysis

The based peak intensity chromatograms (shown in Fig. 1) were obtained from red ginseng at different steaming temperatures in

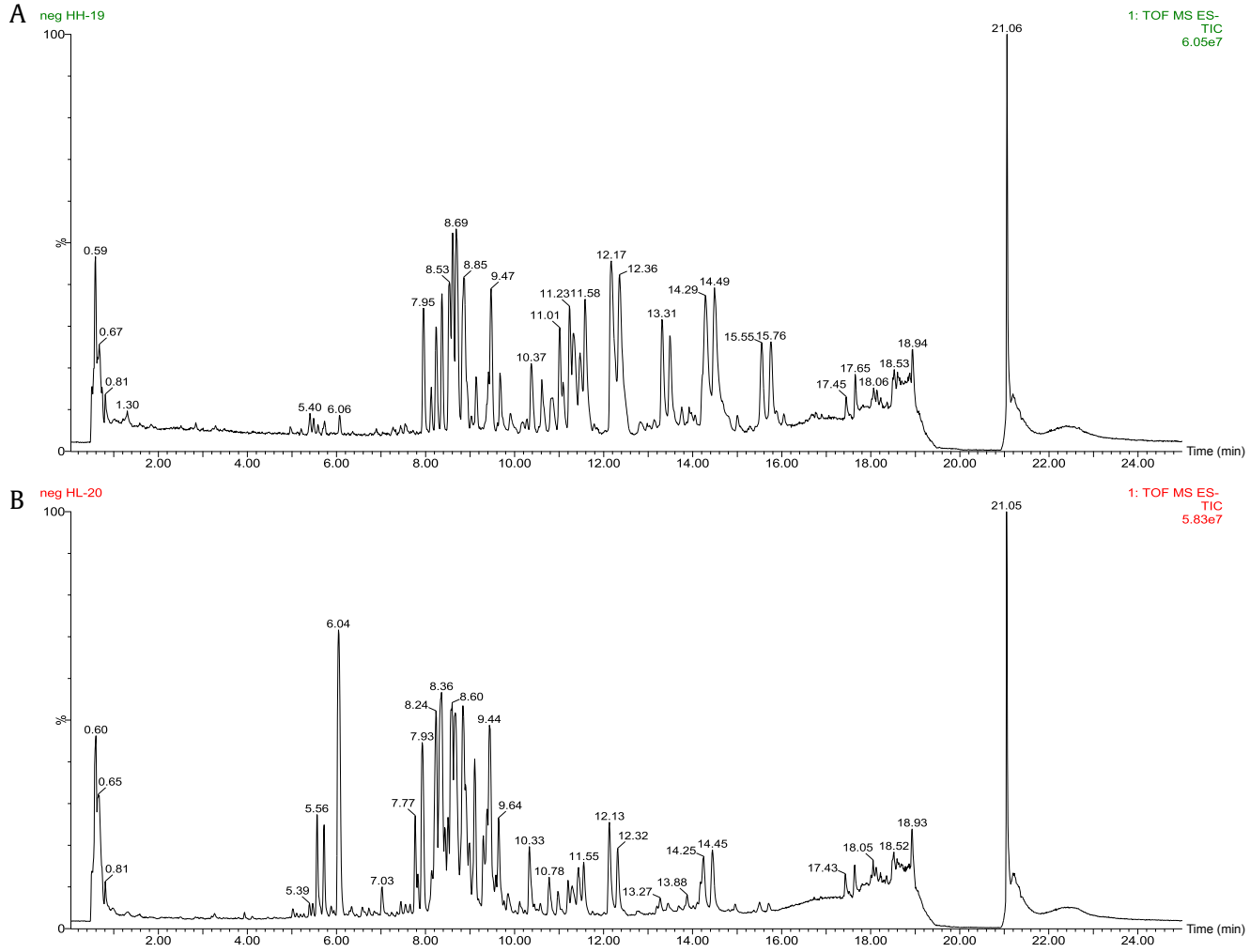

Fig. 1. Representative base peak intensity chromatograms of red ginseng samples. (A) Red ginseng (HH). (B) Red ginseng (HL). ES-, negative electrospray ionization; HH, high temperature; HL, low temperature; neg, negative; TIC, total ion chromatography; TOF MS, time-of-flight mass spectrometry.

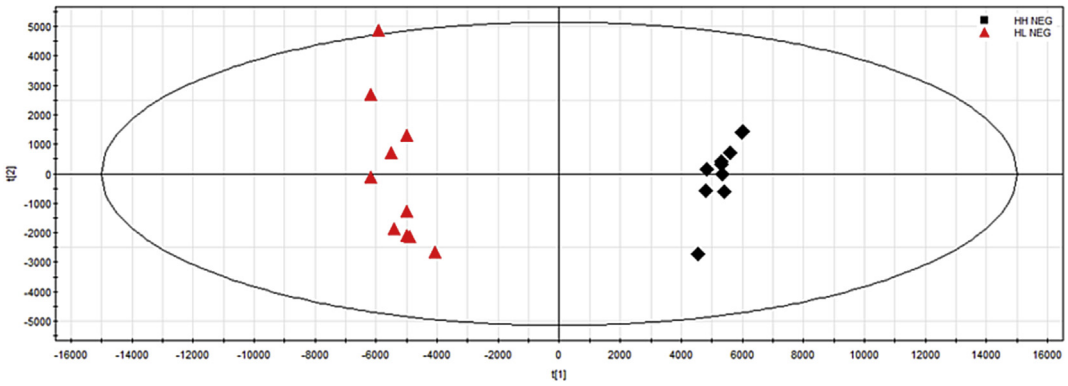

Fig. 2. The PCA of red ginseng at different steaming temperature. PCA, principal component analysis; HH, high temperature; HL, low temperature; NEG: negative ion model.

negative ion mode. The presence of numerous peaks indicated that the components were complex in the sample. Firstly, we can see that polar compounds were the main ingredient of red ginseng steamed at low temperature. By contrast, after high-temperature processing, red ginseng showed an abundant amount of less polar compounds.

3.2. Principal component analysis

We can see the component differences of red ginseng processed at different steaming temperatures from the based peak intensity (shown in Fig. 1). Moreover, MVAs such as PCA and S-plot were used to clearly show the difference and to find the marker ions of red ginseng at different steaming temperatures.

A two-component PCA scores plot of UPLC–QTOF-MS/MS data was used to present the general variation of components among the *P. ginseng* samples (Fig. 2). The PCA scores plot of red ginseng samples in Fig. 2 could be readily divided into two big clusters. The red ginseng samples were clearly separated by principal component 1 (PC1). It appeared that their components were diverse for different processing.

3.3. Marker ions analysis of OPLS-DA

It is evident from Fig. 2 that samples were clustered into two groups: one is red ginseng at low steaming temperature, and the other is red ginseng at high steaming temperature, confirming that the different processing modes indeed influenced the components at levels and occurrence.

To explore the potential chemical markers that contributed most to the differences, UPLC-MS data from red ginseng samples were processed using supervised OPLS-DA. In the S-plot (Fig. 3), each point represents an EMRT pair (a marker), among which the two poles of the "S" curve are right the maker ions. These ions were both further away from the 0 value of *X*-axis and *Y*-axis, which substantially contributed to sample variance and the better correlation from injection to injection. As shown in the S-plot in Fig. 3, the first 12 ions—1 ($t_R = 5.58$ min, m/z 1,077.5450), 2 ($t_R = 6.06$ min, m/z 991.5478), 3 ($t_R = 6.08$ min, m/z 845.4918), 4 ($t_R = 7.95$ min, m/z 845.4921), 5 ($t_R = 8.37$ min, m/z 1,153.6040), 6 ($t_R = 8.47$ min, m/z 1,193.5976), 7 ($t_R = 8.63$ min, m/z 1,123.5930), 8 ($t_R = 8.86$ min, m/z 1,123.5930), 9 ($t_R = 8.88$ min, m/z 1,123.5930), 10 ($t_R = 9.43$ min, m/z 1,165.6030), 11 ($t_R = 9.48$ min, m/z 991.5521), 12 ($t_R = 9.68$ min, m/z 1,165.6040)—at the lower left corner of the "S" were the ions from red ginseng processed at low steaming temperature that contributed most to the differences between red ginseng samples. Analogously, the 15 ions—13 ($t_R = 8.60$ min, m/z 683.4375), 14 ($t_R = 10.40$ min, m/z 827.4811), 15 ($t_R = 10.62$ min, m/z 827.4809), 16 ($t_R = 11.02$ min, m/z 811.4861), 17 ($t_R = 11.24$ min, m/z 811.4862), 18 ($t_R = 11.34$ min, m/z 665.4270), 19 ($t_R = 11.59$ min, m/z 665.4271), 20 ($t_R = 12.18$ min, m/z 829.4970), 21 ($t_R = 12.36$ min, m/z 829.4972), 22 ($t_R = 13.31$ min, m/z 871.5072), 23 ($t_R = 13.49$ min, m/z

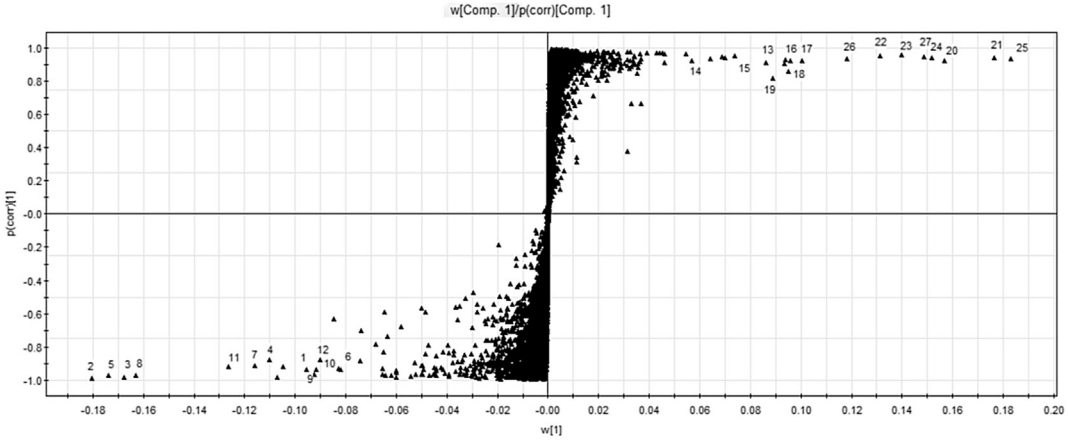

Fig. 3. The S-Plot of red ginseng at different steaming temperature. 1 ion ($t_R = 5.58$ min, m/z 1,077.5450), 2 ion ($t_R = 6.06$ min, m/z 991.5478), 3 ion ($t_R = 6.08$ min, m/z 845.4918), 4 ion ($t_R = 7.95$ min, m/z 845.4921), 5 ion ($t_R = 8.37$ min, m/z 1,153.6040), 6 ion ($t_R = 8.47$ min, m/z 1,193.5976), 7 ion ($t_R = 8.63$ min, m/z 1,123.5930), 8 ion ($t_R = 8.86$ min, m/z 1,123.5930), 9 ion ($t_R = 8.88$ min, m/z 1,123.5930), 10 ion ($t_R = 9.43$ min, m/z 1,165.6030), 11 ion ($t_R = 9.48$ min, m/z 991.5521), 12 ion ($t_R = 9.68$ min, m/z 1,165.6040); 13 ion ($t_R = 8.60$ min, m/z 683.4375), 14 ion ($t_R = 10.40$ min, m/z 827.4811), 15 ion ($t_R = 10.62$ min, m/z 827.4809), 16 ion ($t_R = 11.02$ min, m/z 811.4861), 17 ion ($t_R = 11.24$ min, m/z 811.4862), 18 ion ($t_R = 11.34$ min, m/z 665.4270), 19 ion ($t_R = 11.59$ min, m/z 665.4271), 20 ion ($t_R = 12.18$ min, m/z 829.4970), 21 ion ($t_R = 12.36$ min, m/z 829.4972), 22 ion ($t_R = 13.31$ min, m/z 871.5072), 23 ion ($t_R = 13.49$ min, m/z 871.5073), 24 ion ($t_R = 14.29$ min, m/z 811.4860), 25 ion ($t_R = 14.49$ min, m/z 811.4863), 26 ion ($t_R = 15.54$ min, m/z 853.4965), 27 ion ($t_R = 15.76$ min, m/z 853.4968).

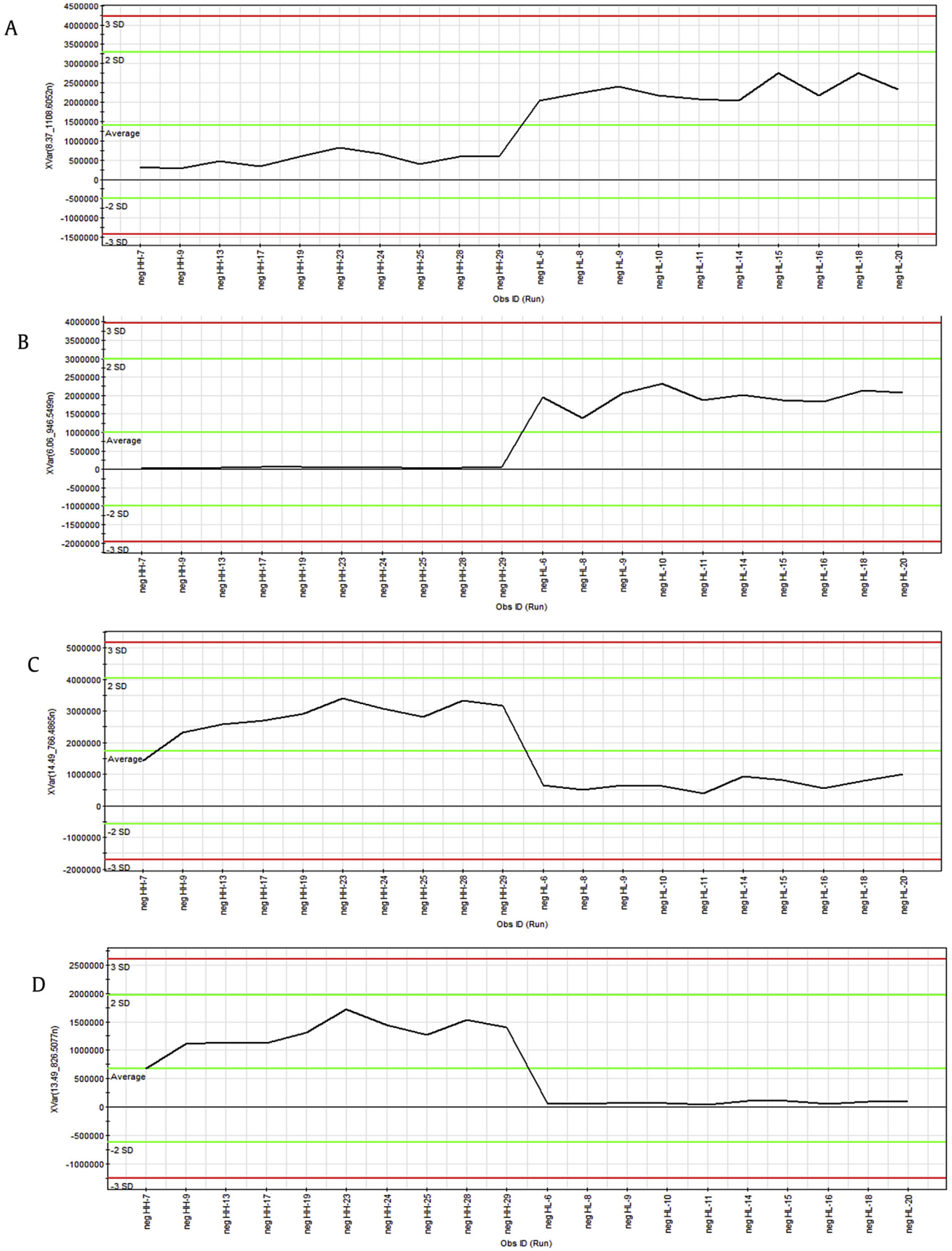

Fig. 4. Representative ion-intensity plot for marker ions over 20 samples. (A) Ginsenoside Rb1 at *m*/*z* 1,153.6040 ($t_R = 8.37$ min). (B) Ginsenoside Re at *m*/*z* 991.5519 ($t_R = 6.06$ min). (C) ginsenoside Rg5 at *m*/*z* 811.4863 ($t_R = 14.49$ min). (D) 20*S*-Ginsenoside Rs3 at *m*/*z* 871.5073 ($t_R = 13.49$ min).

Table 1
Maker ions that were from different processed ginseng

Mark ion	Identification	t_R (min)	Molecular formula	Ion	Mean measured mass	Theoretical exact mass	Mass accuracy (ppm)	Fragment ions	Classification
1	20-Gluco-ginsenoside Rf	5.58	$C_{48}H_{82}O_{19}$	$[M+HCOOH-H]^-$	1,007.5450	1,007.5427	2.3	961,799,637,475	HL
2	Ginsenoside Re	6.06	$C_{48}H_{82}O_{18}$	$[M+HCOOH-H]^-$	991.5519	991.5478	4.1	945,783,637	HL
3	Ginsenoside Rg1	6.08	$C_{42}H_{72}O_{14}$	$[M+HCOOH-H]^-$	845.4918	845.4899	2.3	799,637,475	HL
4	Ginsenoside Rf	7.95	$C_{42}H_{72}O_{14}$	$[M+HCOOH-H]^-$	845.4921	845.4899	2.6	799,637,475	HL
5	Ginsenoside Rb1	8.37	$C_{54}H_{92}O_{23}$	$[M+HCOOH-H]^-$	1,153.6040	1,153.6006	3.0	1107,945,783	HL
6	Malonyl-ginsenoside Rb1	8.47	$C_{57}H_{94}O_{26}$	$[M+HCOOH-H]^-$	1,193.5976	1,193.5955	1.8	1107,1089,945,783	HL
7	Ginsenoside Rc	8.63	$C_{53}H_{90}O_{22}$	$[M+HCOOH-H]^-$	1,123.5930	1,123.5900	2.7	1077,945,783	HL
8	Ginsenoside Rb2	8.86	$C_{53}H_{90}O_{22}$	$[M+HCOOH-H]^-$	1,123.5930	1,123.5900	2.7	1077,945,783	HL
9	Ginsenoside Rb3	8.88	$C_{53}H_{90}O_{22}$	$[M+HCOOH-H]^-$	1,123.5930	1,123.5930	2.7	1077,945,783	HL
10	Ginsenoside Rs1	9.43	$C_{55}H_{92}O_{23}$	$[M+HCOOH-H]^-$	1,165.6030	1,165.6006	2.1	1119,1077,945, 783,621	HL
11	Ginsenoside Rd	9.48	$C_{48}H_{82}O_{18}$	$[M+HCOOH-H]^-$	991.5521	991.5478	4.3	945,783,621	HL
12	Ginsenoside Rs2	9.68	$C_{55}H_{92}O_{23}$	$[M+HCOOH-H]^-$	1,165.6040	1,165.6006	2.9	1119,1077,945,783	HL
13	Ginsenoside Rh1	8.60	$C_{36}H_{62}O_9$	$[M+HCOOH-H]^-$	683.4375	683.4370	0.7	637	HH
14	Ginsenoside Rg8	10.40	$C_{42}H_{70}O_{13}$	$[M+HCOOH-H]^-$	827.4811	827.4793	2.2	987,945,783,621	HH
15	Ginsenoside Rg9	10.62	$C_{42}H_{70}O_{13}$	$[M+HCOOH-H]^-$	827.4809	827.4793	1.9	781,619	HH
16	Ginsenoside Rg6	11.02	$C_{42}H_{70}O_{12}$	$[M+HCOOH-H]^-$	811.4861	811.4844	2.1	765,619	HH
17	Ginsenoside Rg4	11.24	$C_{42}H_{70}O_{12}$	$[M+HCOOH-H]^-$	811.4862	811.4844	2.2	765,619	HH
18	Ginsenoside Rk3	11.34	$C_{36}H_{60}O_8$	$[M+HCOOH-H]^-$	665.4270	665.4265	0.8	619	HH
19	Ginsenoside Rh4	11.59	$C_{36}H_{60}O_8$	$[M+HCOOH-H]^-$	665.4271	665.4265	0.9	619	HH
20	20*S*-Ginsenoside Rg3	12.18	$C_{42}H_{72}O_{13}$	$[M+HCOOH-H]^-$	829.4970	829.4949	2.5	783,621,459	HH
21	20*R*-Ginsenoside Rg3	12.36	$C_{42}H_{72}O_{13}$	$[M+HCOOH-H]^-$	829.4972	829.4949	2.8	783,621,459	HH
22	20*S*-ginsenoside Rs3	13.31	$C_{44}H_{74}O_{14}$	$[M+HCOOH-H]^-$	871.5072	871.5055	2.0	825,783,621,459	HH
23	20*R*-Ginsenoside Rs3	13.49	$C_{44}H_{74}O_{14}$	$[M+HCOOH-H]^-$	871.5073	871.5055	2.1	825,783,621,459	HH
24	Ginsenoside Rk1	14.29	$C_{42}H_{70}O_1$	$[M+HCOOH-H]^-$	811.4860	811.4844	2.0	765,603	HH
25	Ginsenoside Rg5	14.49	$C_{42}H_{70}O_{12}$	$[M+HCOOH-H]^-$	811.4863	811.4844	2.3	765,603	HH
26	Ginsenoside Rs5	15.54	$C_{44}H_{72}O_{13}$	$[M+HCOOH-H]^-$	853.4965	853.4949	1.9	807,765,747,603	HH
27	Ginsenoside Rs4	15.76	$C_{44}H_{72}O_{13}$	$[M+HCOOH-H]^-$	853.4968	853.4949	2.2	807,765,747,603	HH

HH, high temperature; HL, low temperature

871.5073), 24 (t_R = 14.29 min, *m/z* 811.4860), 25 (t_R = 14.49 min, *m/z* 811.4863), 26 (t_R = 15.54 min, *m/z* 853.4965), 27 (t_R = 15.76 min, *m/z* 853.4968)—at the top right corner of the "S" were ions from red ginseng processed at high steaming temperature that contributed most to the differences between red ginseng samples. These ions could be used as potential chemical markers to distinguish the red ginseng that were processed differently.

Moreover, these spectral variables can be further confirmed using the ion intensity plot (Fig. 4) generated by Marker Lynx software for profiling the marker ions. The marker ion t_R = 8.37 min, *m/z* 1,153.6040 (Fig. 4A) and t_R = 6.06 min, *m/z* 991.5519 (Fig. 4B) were from the red ginseng steamed at low temperature. The marker ion t_R = 14.49 min, *m/z* 811.4863 (Fig. 4C) and t_R = 13.49 min, *m/z* 871.5073 (Fig. 4D) were from the red ginseng steamed at high temperature. These representative ions have higher levels in one sample but not in other samples, illustrating the abundance of marker ions over 20 samples.

From the ion intensity plot, we can see the characteristic components in different red ginseng samples. The ion t_R = 5.58 min, *m/z* 1,007.5450; ion t_R = 6.06 min, *m/z* 991.5519; ion t_R = 6.08 min, *m/z* 845.4918; and ion t_R = 8.47 min, *m/z* 1,193.5976 were the unique components of red ginseng steamed at low temperature. Similarly, ion t_R = 13.49 min, *m/z* 871.5073 and ion t_R = 15.76 min, *m/z* 853.4968 were the unique components of red ginseng steamed at high temperature.

Table 2
Determination of ginsenosides in different ginseng products (n = 2, %)

	Rg_1	Re	Rb_1	Rf	Rg_2	Rc	Rb_2	Rb_3	Rg_3
Fresh ginseng	0.175	0.166	0.215	0.093	0.021	0.161	0.078	0.009	—
Red ginseng (HL)	0.587	0.328	1.333	0.300	0.092	0.706	0.797	0.080	0.030
Red ginseng (HH)	—	—	0.304	0.106	0.159	0.075	0.072	0.013	0.338

HH, high temperature; HL, low temperature

3.4. Components assignment

The element composition calculation was performed after acquiring the target markers. The molecular formula of the potential markers can be obtained easily by calculating the accurate masses. The next step was to search against a database and contrast the retention times with correlation references to identify the markers. Finally, the structure of markers can be illuminated by the fragments that appeared in the high capillary electrophoresis scan. The results are presented in Table 1.

By matching the retention times and accurate masses with those of published known compounds, the ions 1–12 in red ginseng samples steamed at low temperature were identified as 20-gluco-ginsenoside Rf, ginsenoside Re, ginsenoside Rg1, ginsenoside Rf, ginsenoside Rb1, malonyl-ginsenoside Rb1, ginsenoside Rc, ginsenoside Rb2, ginsenoside Rb3, ginsenoside Rs1, ginsenoside Rd, and ginsenoside Rs2, respectively.

The ions 13–27 in red ginseng samples steamed at high temperature samples were identified as ginsenoside Rh1, ginsenoside Rg8, ginsenoside Rg9, ginsenoside Rg6, ginsenoside Rg4, ginsenoside Rk3, ginsenoside Rh4, 20*S*-ginsenoside Rg3, 20*R*-ginsenoside Rg3, 20*S*-ginsenoside Rs3, 20*R*-ginsenoside Rs3, ginsenoside Rk1, ginsenoside Rg5, ginsenoside Rs5, and ginsenoside Rs4, respectively.

3.5. Determination of ginsenosides in different ginseng products

We have established a method to determine the ginsenosides Rg_1, Re, Rb_1, Rf, Rg_2, Rb_2, Rc, Rb_3, and Rg_3. The quantitative determination data are shown in Table 2, and the HPLC chromatograms of fresh ginseng and red ginseng steamed at different temperatures are shown in Figs. 5 and 6.

It can be seen that the level of ginsenosides was significantly distinct in different ginseng samples. In comparison with fresh

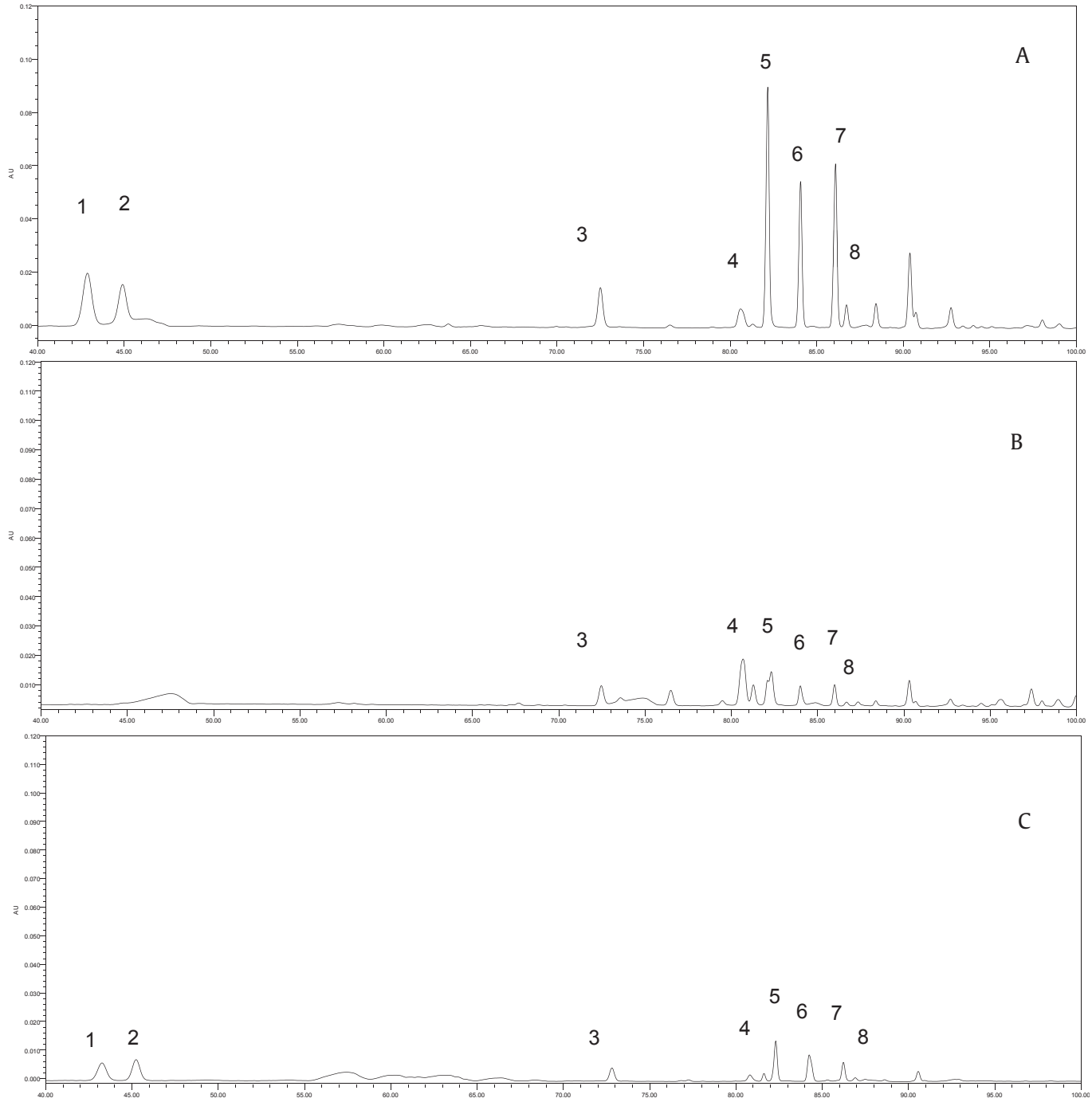

Fig. 5. The HPLC chromatograms of ginseng samples. A: Red ginseng (100°C); B: Red ginseng (120°C); C: Fresh ginseng. (1: Rg_1; 2: Re; 3: Rf; 4: Rg_2; 5: Rb_1; 6: Rc; 7: Rb_2; 8: Rb_3). HPLC, high-performance liquid chromatography.

ginseng, red ginseng (HL) contains a large amount of ginsenosides for demalonylation, deglycosylation, and dehydration. However, red ginseng (HH) can promote these reactions, so ginsenosides Rg_1 and Re were not detected and ginsenoside Rg_3 was found in high level, indicating that temperature indeed influenced the transformation of ginsenosides.

3.6. Chemical change of ginsenoside Rb1 by steaming

In the steaming model experiment, the amount of ginsenoside Rb1 was steamed at 100°C and 120°C, respectively. As shown in Fig. 7, peak 1 and peak 3 were identified by comparing them with standard ginsenosides. However, peak 2, peak 4, and peak 5 were

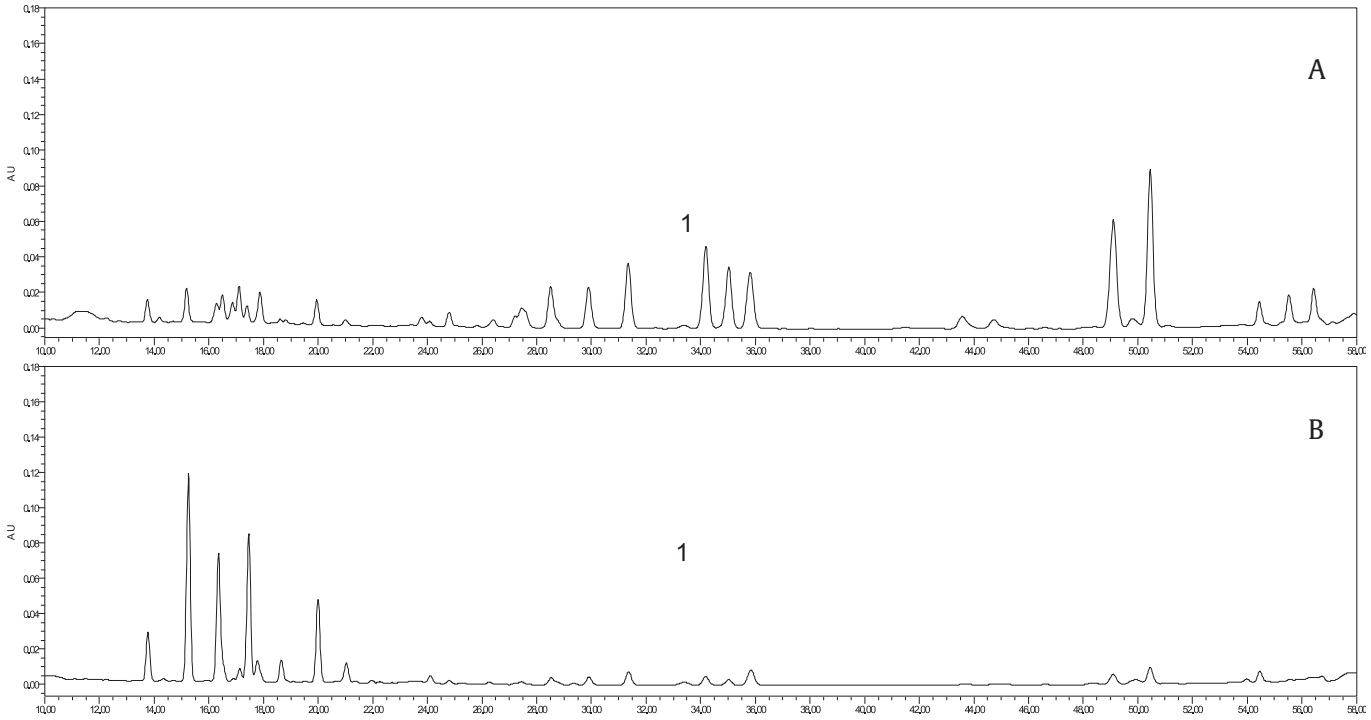

Fig. 6. The HPLC chromatograms of Red ginseng samples. A: Red ginseng (120°C); B: Red ginseng (100°C). (1: Rg_3). HPLC, high-performance liquid chromatography.

assigned by comparing them with related references that were published previously [23,24]. In the steaming model experiment, ginsenoside Rb1 was transformed into 20(*S*)-Rg3, 20(*R*)-Rg3, Rk1, and Rg5 by the steaming process at 120°C for 3 h (Fig. 7B); however, this was not observed during steam processing at 100°C for 3 h (Fig. 7A), as shown by HPLC chromatograms. Although this experiment cannot exactly duplicate the complex reaction in the red ginseng processing, it can indicate that the high steaming temperature can promote the transformation of ginsenosides.

3.7. *Transformation of ginsenosides*

The ginsenosides in red ginseng processed at different steaming temperatures are shown in Figs. 8 and 9. The characteristic

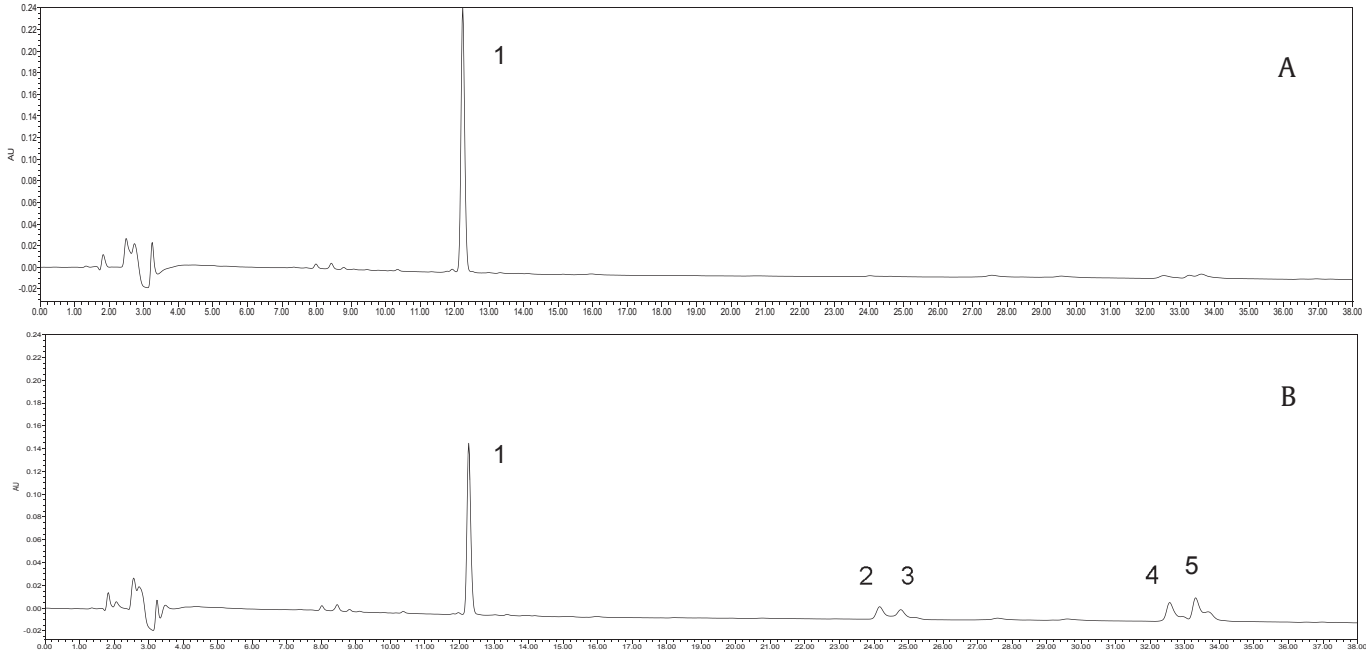

Fig. 7. The changes in HPLC chromatograms of ginsenoside Rb_1 by different steam temperature. A: Red ginseng (100°C); B: Red ginseng (120°C). (1: Rb_1; 2: 20(*S*)-Rg_3; 3: 20(*R*)-Rg_3; 4: Rk_1; 5: Rg_5). HPLC, high-performance liquid chromatography.

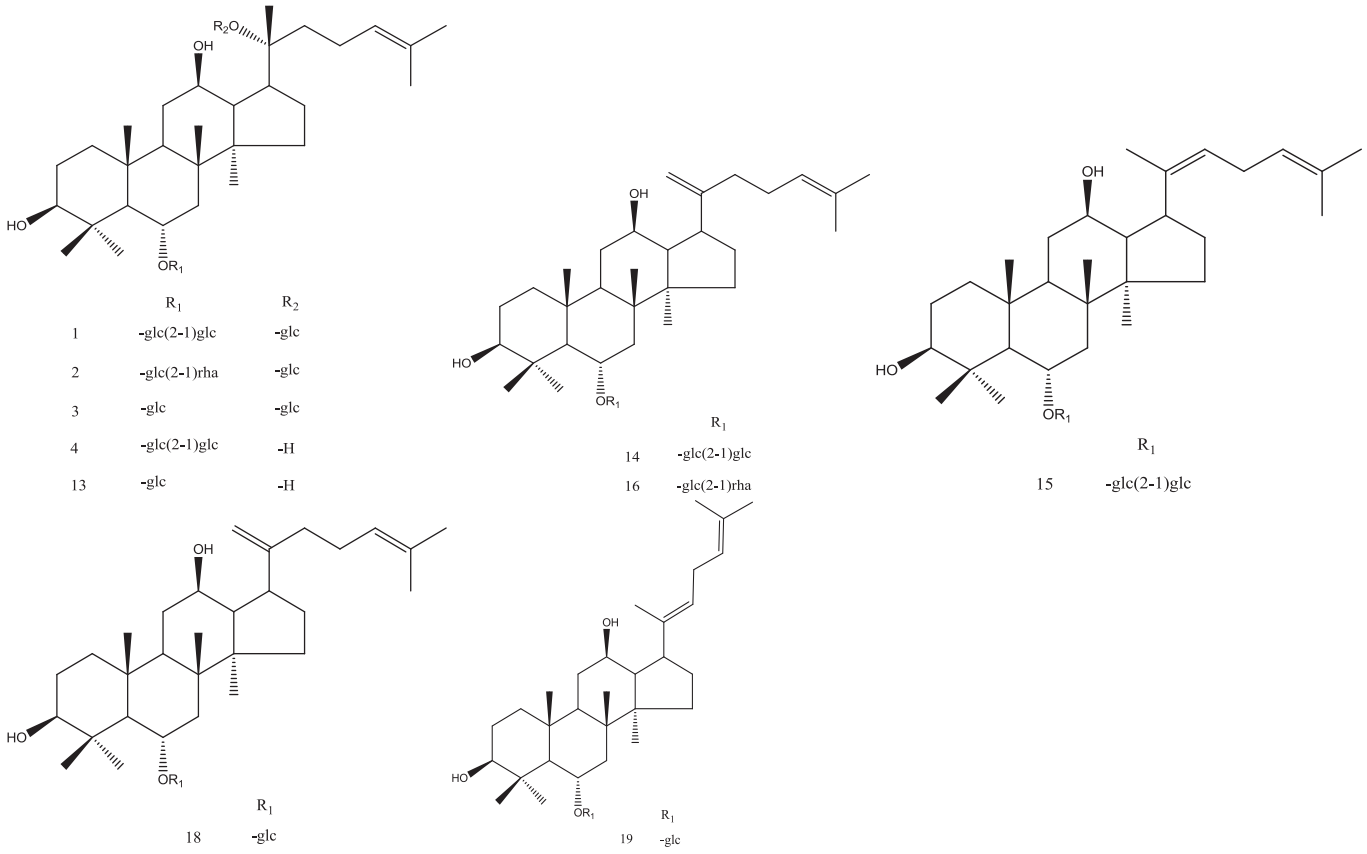

Fig. 8. Structure of protopanaxatriol ginsenoside.

components in red ginseng steamed at low temperature were 20-gluco-ginsenoside Rf, ginsenoside Re, ginsenoside Rg1, and malonyl-ginsenoside Rb1. Meanwhile, the characteristic components in red ginseng steamed at high temperature were 20*R*-ginsenoside Rs3 and ginsenoside Rs4.

During steaming at high temperature, the major ginsenosides can be transformed into rare ginsenosides. The temperature can enhance the chemical reaction of demalonylation, deglycosylation, and dehydration (shown in Fig. 10). The red ginseng samples steamed at high temperature contained an abundant amount of

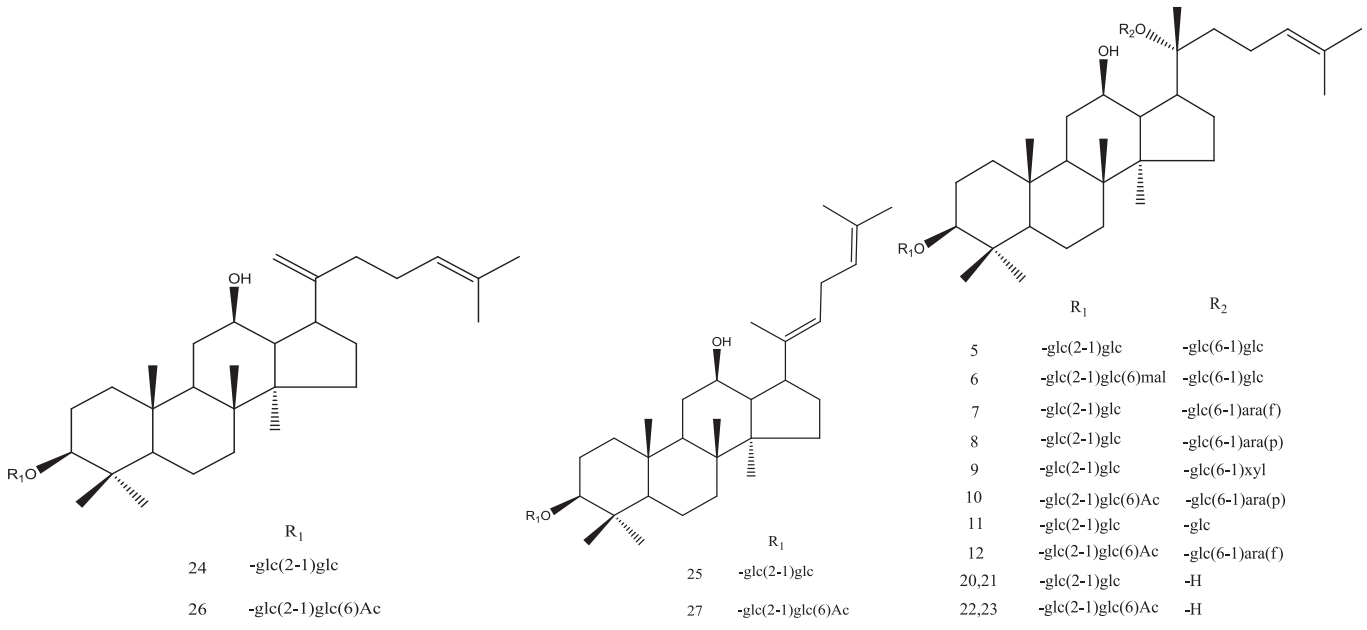

Fig. 9. Structure of protopanaxadiol ginsenoside.

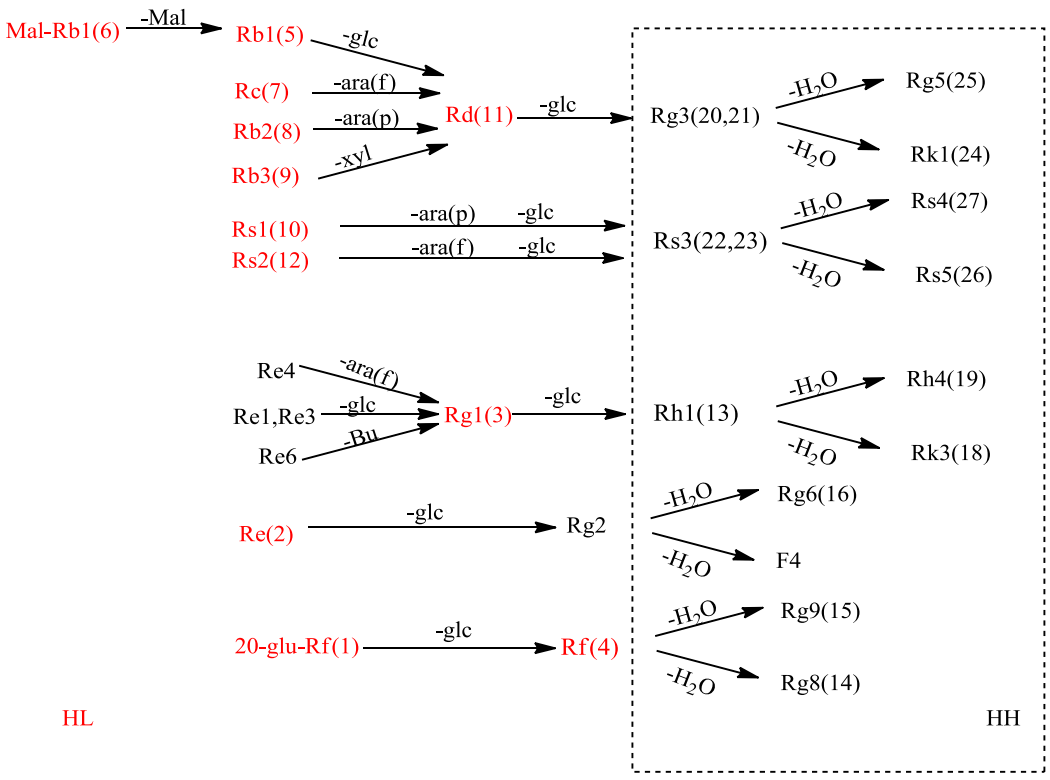

Fig. 10. Transformation of ginsenosides in Red ginseng. HH: high temperature; HL: low temperature. (ara(f): α-L-arabinofuranosyl; ara(p): α-L-arabinopyranosyl; rha:α-L-arabinopyranosyl; glc: β-D-glucopyranosyl; xyl: β-D-xylopyranosyl; Mal: malonyl; Bu: *trans*-but-2-enoyl).

rare ginsenosides, which have greater pharmacological activity in the clinic.

Malonyl-ginsenosides are natural products in fresh ginseng. When fresh ginseng is processed into red ginseng, ginsenosides can demalonylate, decarboxylate, deglycosylate, and dehydrate into other ginsenosides. Among these reactions, demalonylation and decarboxylation occur easily, and then deglycosylation and dehydration occur in position 20 of the dammarane skeleton. The ether bond is stable at positions 3 and 6 in the dammarane skeleton, and which between sugars in this position is also stable. The red ginseng steamed at low temperature was mainly involved demalonylation, decarboxylation, and the first deglycosylation in 20 of dammarane skeleton. However, the red ginseng steamed at high temperature promoted these reactions and was mainly conducted via the second deglycosylation in 20 of dammarane skeleton and dehydration in this position. The elucidation of ginsenosides transformation was consistent with the outcome of MVA and the determination of ginsenosides.

4. Conclusion

MAV and UPLC–QTOF-MS/MS were combined to analyze the multiple groups of complex samples. This combination focused on the details of the samples so that many important marker ions could be measured even at low concentration levels. As a result, the steam temperature can enhance the transformation of ginsenosides via demalonylation, deglycosylation, and dehydration. This is the first study to reveal the ginsenosides transformation in red ginseng at different steaming temperatures and observe the transformation of ginsenosides at the chemical component level.

Conflicts of interest

The authors declare that there are no conflicts of interest regarding the publication of this paper.

Acknowledgments

This study was supported by grants from the National Natural Science Foundation of China (no. 81073041) and the Specialized Research Fund for the Doctoral Program of Higher Education of China (no. 20100013120010).

References

[1] Kennedy DO, Scholey AB. Ginseng: potential for the enhancement of cognitive performance and mood. Pharmacol Biochem Behav 2003;75:687–700.
[2] Coleman CI, Hebert JH, Reddy P. The effects of *Panax ginseng* on quality of life. J Clin Pharm Ther 2003;28:5–15.
[3] Jiao L, Zhang X, Wang M, Li B, Liu Z, Liu S. Chemical and antihyperglycemic activity changes of ginseng pectin induced by heat processing. Carbohydr Polym 2014;114:567–73.
[4] Yang WZ, Ye M, Qiao X, Liu CF, Miao WJ, Bo T, Tao HY, Guo DA. A strategy for efficient discovery of new natural compounds by integrating orthogonal column chromatography and liquid chromatography/mass spectrometry analysis: its application in *Panax ginseng, Panax quinquefolium* and *Panax notoginseng* to characterize 437 potential new ginsenosides. Anal Chim Acta 2012;739:56–66.
[5] Wang Y, Chen Y, Xu H, Luo H, Jiang R. Analgesic effects of glycoproteins from *Panax ginseng* root in mice. J Ethnopharmacol 2013;148:946–50.
[6] Kim YK, Guo Q, Packer L. Free radical scavenging activity of red ginseng aqueous extracts. Toxicology 2002;172:149–56.
[7] Bu HB, Wang F, Lin HY, Guo ZY, Yuan SX, Pan LL, Xu XJ, Li XR, Wang GL, Lin RC. Nondestructive recognization of mountain cultivated ginseng and garden cultivated ginseng by FTIR microspectroscopy. Spectrosc Spect Anal 2013;33:3028–31.

[8] Zhang HM, Li SL, Zhang H, Wang Y, Zhao ZL, Chen SL, Xu HX. Holistic quality evaluation of commercial white and red ginseng using a UPLC-QTOF-MS/MS-based metabolomics approach. J Pharm Biomed Anal 2012;62:258–73.
[9] Kim YJ, Choi WI, Jeon BN, Choi KC, Kim K, Kim TJ, Ham J, Jang HJ, Kang KS, Ko H. Stereospecific effects of ginsenoside 20-Rg3 inhibits TGF-β1-induced epithelial–mesenchymal transition and suppresses lung cancer migration, invasion and anoikis resistance. Toxicology 2014;322:23–33.
[10] Li B, Zhao J, Wang CZ, Searle J, He TC, Yuan CS, Du W. Ginsenoside Rh2 induces apoptosis and paraptosis-like cell death in colorectal cancer cells through activation of p53. Cancer Lett 2011;301:185–92.
[11] Lin Y, Jiang D, Li Y, Han X, Yu D, Park JH, Jin YH. Effect of sun ginseng potentiation on epirubicin and paclitaxel-induced apoptosis in human cervical cancer cells. J Ginseng Res 2014;39:856–64.
[12] Lee CH, Kim JM, Dong HK, Park SJ, Liu X, Mudan C, Jin GH, Park JH, Ryu JH. Effects of Sun ginseng on memory enhancement and hippocampal neurogenesis. Phytother Res 2013;27:1293–9.
[13] Li J, Zhong W, Wang W, Hu S, Yuan J, Zhang B, Hu T, Song G. Ginsenoside metabolite compound K promotes recovery of dextran sulfate sodium-induced colitis and inhibits inflammatory responses by suppressing NF-κB activatio. Plos One 2014;9:e87810.
[14] Zhang YX, Wang L, Xiao EL, Li SJ, Chen JJ, Gao B, Min GN, Wang ZP, Wu YJ. Ginsenoside-Rd exhibits anti-inflammatory activities through elevation of antioxidant enzyme activities and inhibition of JNK and ERK activation in vivo. Int Immunopharmacol 2013;17:1094–100.
[15] Dong H, Bai LP, Wong VK, Zhou H, Wang JR, Liu Y, Jiang ZH, Liu L. The in vitro structure-related anti-cancer activity of ginsenosides and their derivatives. Molecules 2011;16:10619–30.
[16] Chen F, Chen Y, Kang X, Zhou Z, Zhang Z, Liu D. Anti-apoptotic function and mechanism of ginseng saponins in *Rattus* pancreatic β-cells. Biol Pharm Bull 2012;35:1568–73.
[17] Choi YJ, Kang LJ, Lee SG. Stimulation of DDX3 expression by ginsenoside Rg3 through the Akt/p53 pathway activates the innate immune response via TBK1/IKKε/IRF3 signalling. Curr Med Chem 2014;21:1050–60.
[18] Xu XF, Nie LX, Pan LL, Hao B, Yuan SX, Lin RC, Bu HB, Wang D, Dong L, Li XR. Quantitative analysis of *Panax ginseng* by FT-NIR spectroscopy. J Anal Methods Chem 2014;2014:1087–100.
[19] Ying W, Zhao W, Qi Z, Zhao Y, Zhang Y. Purification and characterization of a novel and unique ginsenoside Rg1-hydrolyzing β-d-glucosidase from *Penicillium sclerotiorum*. Acta Biochim Biophy Sin 2011;43:226–31.
[20] Kim N, Kim K, Lee D, Shin YS, Bang KH, Cha SW, Lee JW, Choi HK, Hwang BY, Lee D. Nontargeted metabolomics approach for age differentiation and structure interpretation of age-dependent key constituents in hairy roots of *Panax ginseng*. J Nat Prod 2012;75:1777–84.
[21] Song HH, Moon JY, Ryu HW, Noh BS, Kim JH, Lee HK, Oh SR. Discrimination of white ginseng origins using multivariate statistical analysis of data sets. J Ginseng Res 2014;38:187–93.
[22] Xie YY, Luo D, Cheng YJ, Ma JF, Wang YM, Liang QL, Luo GA. Steaming-induced chemical transformations and holistic quality assessment of red ginseng derived from *Panax ginseng* by means of HPLC-ESI-MS/MS(n)-based multicomponent quantification fingerprint. J Agric Food Chem 2012;60:8213–24.
[23] Kang KS, Kim HY, Baek SH, Yoo HH, Park JH, Yokozawa T. Study on the hydroxyl radical scavenging activity changes of ginseng and ginsenoside-Rb2 by heat processing. Biol Pharm Bull 2007;30:724–8.
[24] Lee W, Park SH, Lee S, Chung BC, Song MO, Song KI, Ham J, Kim SN, Kang KS. Increase in antioxidant effect of ginsenoside Re-alanine mixture by Maillard reaction. Food Chem 2012;135:2430–5.